EFFECT OF γ-RADIATION AND CHARACTERIZATION OF SYNTHESIZED BENZYLIDINE PHENYLTHIAZOLE AMINES AND SOME METAL-COMPLEX DERIVATIVES

R. O. ALY[1], R. S. FARAG[2], M. M. HASSAN[2]
1-National Center for Radiation Research and Technology, Nasr City, Cairo, Egypt
2- Chemistry Department, Faculty of Science, Al-Azhar University, Nasr City, Cairo, Egypt

Abstract

The Schiff-bases, I, II, III were prepared essentially by the condensation reaction between an amine, namely 2-amino-4-phenylthiazole, and an aldehyde: benzaldehyde (I), p-chlorobenzaldehyde (II) and p-nitrobenzaldehyde (III) in 1:1 molar ratio. The metal-complexes of Fe^{3+}, Co^{2+}, Ni^{2+}, Cu^{2+}, Zn^{2+} and La^{3+} were also synthesized. The structure elucidation was based on: elemental analysis, IR, UV-Visible, ^{1}H NMR and MS spectral analyses.

The impact of γ-radiation on the synthesized compounds was discussed via the post-radiation UV-Visible aftermaths. Some radiolysis products were postulated with the assistance of the obtained MS results. The thermal properties of the metal chelates were confirmed by the means of TGA results. The molar conductance of the derivatives supported the 1:1 and 1:2 electrolyte behaviors.

Metal-complex magnetic behavior in association with the UV-Visible data suggested the octahedral for all complexes except III_b is tetrahedral arrangement, whereas, Cu-complexes demonstrated distorted geometry. Furthermore, the Cu-complex of the ligand III_d proved to be very highly active against the Gram-positive Bacillus *subtilis* (NCTC-1040), whereas Co-complex of II_b showed significant inhibition, similarly on Streptococcus *pyogense* (ATCC-19615) and on the fungus Aspergillus *fungatus*.

Keywords: Schiff-base, metal-complex, spectral analysis, γ-irradiation, antimicrobial activity

Introduction

The twentieth century has been characterized both by a drastic reduction in the mortality caused by infectious diseases and by a rise in the control of neoplastic pathologies. Nevertheless, microorganisms and viruses, on the one hand, and tumors, on the other, still represent a dreadful menace to men’s health and therefore, for a more efficient control, require the steady development of novel and more powerful drugs [(1-6)].

Chemists have reported on the chemical, structural and biological properties of Schiff-bases, which are characterized by the -N=CH-, azomethine group [(7-12)]. Vicini et al.[(13)] synthesized different compounds bearing an azomethine linkage and evaluated *in-*

vitro their antiviral, antimicrobial and antiproliferative activities with the aim of identifying lead compounds active against emergent and re-emergent human and cattle infectious diseases, e.g. AIDS, hepatitis B and C, tuberculosis, bovine viral diarrhea, or against drug-resistant cancers, e.g. leukaemia, carcinoma, melanoma, MDR tumors, for which no definitive cure or efficacious vaccine is available at present.

Metal complexes of Schiff-bases derived from substituted salicylaldehyde and heterocyclic compounds containing nitrogen, sulphur and/or oxygen atoms as ligands are of interest as simple structural models of more complicated biological systems [14-16]. Chiral ligands were prepared by the condensation of salicylaldehyde or 5-t-butylsalicylaldehyde with 1, 2-diaminocyclo-hexane in ethanol [17, 18]. Metal salen complexes were prepared by the treatment of the ligands with Cu^{2+} or Ni^{2+} salts. Mercury, as one of the most hazardous heavy metals in the environment, can be potentially removed by salen metal complexes for environmental remediation and the resultant bimetallic complexes may be used as chiral mercury reagents.

The interest in transition metal-complexes of Schiff-bases continues not only due to the interesting structural and bonding modes they possess but also due to synthetic flexibility, selectivity and sensitivity towards the central metal atom in addition to their varied industrial applications [19, 20].

In the present work three Schiff bases were prepared by the condensation reaction between the aromatic amine 2-amino-4-phenylthiazole and aldehydes, namely benzaldehyde, p-chlorobezaldehyde and p-nirtro benzaldehyde. Some ligand metal-complexes were synthesized and characterized by physicochemical and spectral analyses. Some title compounds were subjected to γ-radiation and further spectral investigation was performed.

Experimental

Materials

All the employed chemicals were Merck-Germany, products. The Schiff- base implemented amine is 2-amino-4-phenylthiazole and the applied aldehydes are benzaldehyde, p-chlorobenzaldehyde and p-nitrobenzaldehyde. Metal-complexes were prepared by using the metal salts: $Fe(NO_3)_3.9H_2O$, $Co(CH_3COO)_2.4H_2O$,

$Ni(CH_3COO)_2.4H_2O$, $Cu(CH_3COO)_2.H_2O$, $Zn(CH_3COO)_2.2H_2O$ and $LaCl_3.7H_2O$. Solvents and other used chemicals were of highly pure grade.

Instruments

The IR spectra were recorded by Perkin Elmer 57928 RXIFT-IR system. Electronic absorption measurements were performed by Perkin Elmer lambda 35 UV- Visible spectrophotometer. The ^1H NMR spectra were carried out by Varian, Gemini 200 MHz spectrometer. Hewlett Packard MS 5988 spectrometer was used for mass spectrometry. Thermal analysis was applied by Shimadzu 50. Gamma-cell 220A was used for irradiation processes. Conductance Engineered System, U.S.A, was employed for the conductometric titration and molar conductance measurements.

Conductometric measurements

Further insight concerning the structure of these products was gleaned from a consideration of conductometric measurements. Thus, the conductometric titration is performed by titrating 25 ml of $1x10^{-3}$ M metal ion solution with increasing volume of $1x10^{-3}$ M complexing agent solution (Schiff-base derivatives) and the conductance is then recorded after stirring the solution for about 2 min.

By plotting the conductance value, after correction for dilution as a results of addition of chelating agent, VS milliliters of the reagent added applying the least square equation for Y values according to the following equation(21)

$$Y= m X + b$$

where Y is one variable, X is the other, m is the slope of curve and b is the intercept on the ordinate (y axis) Y usually the measured variable plotted as a function of changing as shown in Figs (1). The titration curves are smooth straight lines for all the points, and the well defined breaks are coincident with the steochiometric ratio of complexes formed in solution. The data are in good agreement with the (1:1) molar ratio suggested for these adducts.

The UV absorbance of the mixed solutions was recorded at 302,300,306,276,307 and 316 nm for Fe^{3+}, Co^{2+}, Ni^{2+}, Cu^{2+}, Zn^{2+} and La^{3+}, respectively.

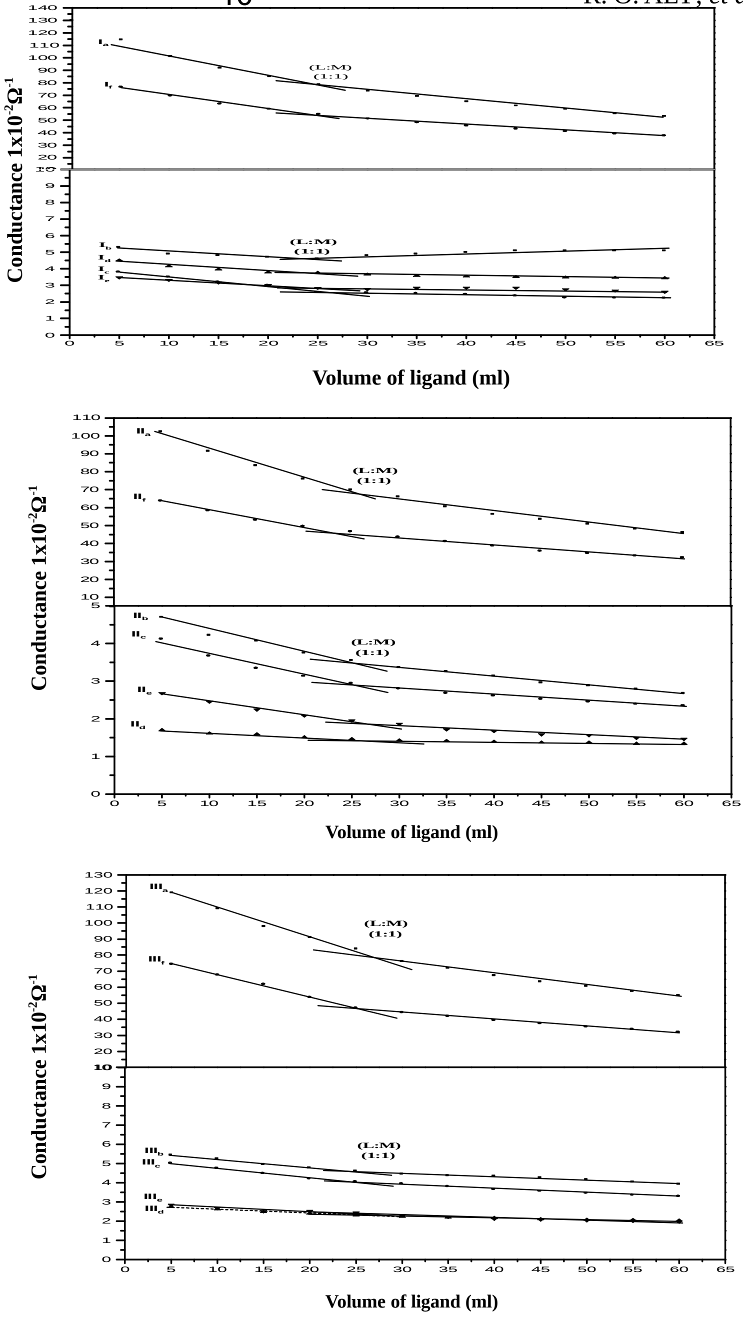

Fig.(1) Conductomeric titration curves for (I_{a-f}_III_{a-f})

The Schiff-bases (I-III) were prepared by condensation reaction in which the aldehyde, 0.1 mole, was dropwisely added to the amine, 0.1 mole, with continuous stirring. Thereafter, the reaction mixture was heated at 100°C for about 10 min in presence of 5 ml ethanol or acetic acid. The isolated yields were purified by recrystallization from a solvent, which gave analytical data see Table (1).

Table (1): Analytical and physical data of Schiff-bases (I-III):

Compd. No.	Products						
	Color	M.P. °C	M. F. M.Wt.	Elemental analysis Calcd. / Found			
				C %	H %	N %	S %
I	Yellowish brown	160-162	$C_{16}H_{12}N_2S$ 264	72.7 71.2	4.58 4.70	10.6 10.5	12.1 11.9
II	Yellow	122-125	$C_{16}H_{11}ClN_2S$ 298	64.3 63.6	3.71 3.42	9.38 9.45	10.7 10.9
III	Reddish yellow	190-192	$C_{16}H_{11}N_3O_2S$ 309	62.1 61.3	3.58 3.84	13.5 12.9	10.3 10.2

Metal-complexes were prepared by the addition of the equimolar amounts of metal salt solution, 0.004 mole, to the Schiff-bases 0.004 moles in 25 ml ethanol. Thereafter, the reaction mixture was heated under reflux for 6 h. The solvent was then allowed to evaporate at room temperature and the obtained solid was filtered and washed with dry ethyl ether, Table (2).

A complementary study based on the electronic absorption spectra and the magnetic moment measurement of metal-complex, via Faraday method[22], was employed to envisage the coordination geometry. The UV-Visible absorption within, λ_{max} = 200-1100 nm, was examined for DMF 10^{-5} M solutions in the UV- and 10^{-3} M in the Visible- sector at room temperature. Meanwhile the molar conductance of metal-complexes was detected in 10^{-3} M DMF solutions at room temperature.

Irradiation process were carried out for 10^{-5} M in the UV- sector and 10^{-3} M in the Visible-sector DMF of selected synthesized substances by an integral gamma dose of 30 kGy at a dose rate of 1.2 Gy s^{-1} under ambient conditions. The post- radiation aftermath was followed up by UV-Visible spectral analysis at the above mentioned concentrations. The synthesized compounds were also tested for the antimicrobial activity using ampicillin as a reference [23].

Table (2): Analytical and physical data of Schiff-base complexes (I-III):

Compd. No.	Product				
	Color	M.P. °C	M. F.	Elemental analysis Calcd. / Found	
				N %	M %
I_a	Dark brown	223-225	$C_{16}H_{14}FeN_5O_{10}S$	13.36 12.85	10.65 11.63
I_b	Violet	325-327	$C_{20}H_{22}CoN_2O_6S$	5.87 5.21	12.34 11.78
I_c	Grey	> 360	$C_{20}H_{22}N_2NiO_6S$	5.87 5.03	12.30 11.63
I_d	Brown	260-262	$C_{20}H_{22}CuN_2O_6S$	5.81 4.60	13.18 12.7
I_e	Dark yellow	197-200	$C_{20}H_{22}N_2O_6SZn$	5.79 5.64	13.52 13.07
I_f	Pale White	232-235	$C_{16}H_{14}Cl_3LaN_2OS$	5.31 5.52	26.33 23.15
II_a	Dark brown	> 360	$C_{16}H_{13}ClFeN_5O_{10}S$	12.54 11.34	10.00 9.28
II_b	Pale violet	257-260	$C_{20}H_{21}ClCoN_2O_6S$	5.47 4.61	11.51 10.31
II_c	Green	163-165	$C_{20}H_{21}ClN_2NiO_6S$	5.48 5.32	11.47 10.27
II_d	Greenish yellow	310-313	$C_{20}H_{21}ClCuN_2O_6S$	5.42 5.09	12.30 11.91
II_e	Pale white	210-212	$C_{20}H_{21}ClN_2O_6SZn$	5.40 4.93	12.62 11.44
II_f	Pale white	320-322	$C_{16}H_{13}Cl_4LaN_2OS$	4.98 4.59	24.71 23.61
III_a	Dark brown	>360	$C_{16}H_{13}FeN_6O_{12}S$	14.76 13.86	9.81 8.97
III_b	Greenish brown	225-228	$C_{20}H_{21}CoN_3O_8S$	8.08 7.25	11.28 10.64
III_c	Dark yellow	220-222	$C_{20}H_{21}N_3NiO_8S$	8.05 7.64	11.24 10.27
III_d	Brown	243-245	$C_{20}H_{21}CuN_3O_8S$	7.97 7.43	12.06 11.12
III_e	Pale yellow	225-227	$C_{20}H_{21}N_3O_8SZn$	7.95 7.79	12.37 11.44
III_f	Greenish yellow	235-237	$C_{16}H_{13}Cl_3LaN_3O_3S$	7.34 7..45	24.26 23.15

Results and Discussion

Schiff-base structural analysis

Elucidation of the chemical structures of the prepared Schiff-bases (I-III) were based on the elemental, Table 1, IR, UV, NMR and MS spectral analyses.

IR – spectra

The stretching vibration bands of the Schiff-bases I, II and III, respectively, are assigned as follows: 3060, 3086 and 3062 cm^{-1} for the stretching vibrations of the aromatic C-H bands; 1610, 1602 and 1602 cm^{-1} for vN=C; 1526, 1526 and 1520 cm^{-1} for vC=C; 1326, 1330 and 1336 cm^{-1} for vC-N; 766, 774 and 768 cm^{-1} for vC-S-C. The weak stretching bands at 2973 and 2865 cm^{-1} of II, and at 2944 and 2858 cm^{-1} of III are ascribed to the δC-H stretching vibration mode of the azomethine group. The deformation mode of the vibration bands at 1402 and 1488 cm^{-1} are accounted for the C-H bond and the band located at 824 cm^{-1} can be attributed to the vC-Cl in II. Meanwhile, the band at 768 cm^{-1} can be referred to the out-of-plane deformation of the C-H bond of the 1, 4-disubstituted benzene ring in III. The IR frequencies are listed in Table (3)

Table 3: Characteristic IR stretching vibration (cm^{-1}) of Schiff-bases (I-III)

Compd. No.	Stretching vibration (υ) in cm^{-1}					
	υC-H_{Ar}	υC-H_{Al}	υC=N	υC=C	υC-N	*υC-S-C*
I	3060	2929	1610	1526	1326	766
II	3086	2973 2865	1602	1526	1330	774
III	3062	2944 2858	1602	1520	1336	768

UV- Electronic absorption spectra

The electronic absorptions of the Schiff-bases I, II and III, respectively, revealed the following results: the regions of λ_{max} = 203-245, 203-244 and 203-244 nm exhibit the structures of the phenyl ring transition ($^1L_a \leftarrow {}^1A$); λ_{max} = 259, 255 and 255 nm of the phenyl ring transition ($^1L_b \leftarrow {}^1A$); λ_{max} = 270, 272 and 272 nm of the π-π* transition in the C=N group; and λ_{max} = 329, 330 and 330 nm of the broad n-π* transition of the N=C in I and II, in addition to N=O group in III. Signal absorptions are listed in Table (4)

Table 4: The electronic absorption spectra of Schiff-bases (I-III)

Compd. No.	Electronic Absorption λ in nm				
	$^1L_a \leftarrow {}^1A$	$^1L_b \leftarrow {}^1A$	π-π^* C=N	n- π^* C=N	n-π^* N=O
I	203-245	259	270	329	-----
II	203-244	255	272	330	-----
III	203-244	259	272	330	330

^{1}H NMR – spectra

The ^{1}H NMR of the three Schiff-bases in DMSO-d_6 demonstrated multiplet signals within the range δ 7-8 attributed to the aromatic protons of two different phenyl rings. A common shift at δ 5.7 in I and II, and at δ 5.8 in III is ascribed to the thiazole ring proton. The azomethine proton is represented at δ 9 in I and II, and δ 8.4 in III. A singlet appeared at δ 7.3 exhibiting the absorption of the phenyl protons in the Cl- substituted aromatic ring in II.

The MS- spectra

The mass spectra of the three Schiff-bases I, II and III displayed the followings:

The molecular peak is respectively as follows for I, II and III: 264 (40.8%), 298 (42.4%) and 309 (24.6%). Two common ion peaks are m/e = 77 with 30.3%, 29.4% and 23.8% and m/e =89 with 43.7%, 78.8% and 47.8%, respectively, corresponding to M^+ (C_6H_5) and M^+ (C_7H_5), respectively. The base peaks are assigned respectively as follows: m/e =134 (100%), 133 (100%) and 175 (100%) representing in order the ions M^+ (C_8H_6S), M^+ (C_8H_6S) and M^+ ($C_9H_7N_2S$). For I, the ion peaks m/e = 176 (83.8%) and 102 (24.8%) are accounted for M^+ ($C_9H_7N_2S$) and M^+ (C_8H_6). For II, the ion peaks m/e = 262 (32.9%), 221 (32.9%), 175 (87.1%) and 101 (52.9%) represent in order the ions M^+ ($C_{16}H_{11}N_2S$), M^+ ($C_{10}H_6Cl\ N_2S$), M^+ ($C_9H_7N_2S$) and M^+ (C_8H_5). For III, the ion peaks m/e = 263 (4.6%), 175 (100%), 133 (93.3%) and 101 (33.1%) are due in order to M^+ ($C_{16}H_{11}N_2S$), M^+ ($C_9H_7N_2S$), M^+ (C_8H_6S) and M^+ (C_8H_5).

The elemental and spectral analyses may corroborate the I, II and III structures as follows:

where, R is C_6H_5 in I : N-bezylidene-5-phenylthaizol-2-amine, *p*-Cl-C_6H_4- in II : N-(4-chlorobenzylidene)-5-phenylthiazol-2-amine and *p*-NO_2-C_6H_4 in III : N-(4-nitrobenzylidene)-5-phenylthiazol-2-amine.

Metal-complex structural analysis

Six metal-complexes were prepared for each synthesized Schiff-base: I_{a-f}, II_{a-f} and III_{a-f} employing the metal ions Fe^{3+}, Co^{2+}, Ni^{2+}, Cu^{2+}, Zn^{2+} and La^{3+}, respectively. The structure recognition was based on the elemental, Table (2), and spectral analyses.

IR- spectra

Comparing the common bands, it is observed that the complex bands shift to lower or higher frequency. Furthermore, metal-nitrogen bonds were found common in the prepared coordination compounds.

For I_{a-f}, with respect to the order of metal ions, the weak broad bands at 3348, 3490, 3490, 3310, 3306 and 3280 cm^{-1} were attributed to the associated water molecules. The weak bands observed at 2940, 2938, 2937, 2935,2927 and 2957 cm^{-1} were ascribed to the starching vibrations of the aliphatic C-H bond in the azomethine, and the acetate groups in Co, Ni, Cu and Zn metal-complexes. Also, the bands located at 1516, 1542, 1570, 1594, 1540 and 1534 cm^{-1} were assigned for *v*C=N bond in the azomethine group which shift to lower frequency than that of the ligand asserting the nitrogen atom participation in the coordination sphere. The acetato complexes displayed also the asymmetric *v*COO^- at 1605, 1590 and 1632 cm^{-1} and the symmetric *v*COO^- at 1342, 1330 and 1382 cm^{-1} in Co, Cu and Zn metal-complexes, respectively[(24)]. The weak bands appeared at 3086, 3098, 3028, 3065, 3098 and 3102 cm^{-1} were ascribed to the starching vibrations of the aromatic C-H bond which demonstrated also in-plane bending deformation bands at 1392, 1408, 1410, 1480, 1440 and 1442 cm^{-1}. The *v*C-S-C bonds were represented by the bands at 690, 676, 684, 698, 694 and 700 cm^{-1}. The observed bands at 610, 616, 618, 624, 529 and 548 cm^{-1}, were accounted for $M \leftarrow N$ coordination bond.

Analogous elucidation was applied for II_{a-f} and III_{a-f} metal-complexes. For II_{a-f}, with respect to the order of metal ions, the weak broad bands at 3364, 3496, 3358, 3374, 3316 and 3300 cm^{-1} were referred to the coordinated water molecules. The weak bands observed at 2955, 2975, 2968, 2948, 2937 and 2960 cm^{-1} were assigned for the starching vibrations of the aliphatic C-H bond of the azomethine, and the acetate groups in Fe, Co, Ni, Cu, Zn and La metal-complexes. The azomethine νC=N bond showed similar responses as that of I_{a-f} at 1518, 1528, 1526,1507, 1482, and 1536 cm^{-1}. Co, Ni, Cu and Zn acetate groups gave ν_{as} COO^- and ν_{sym} COO^- bands at 1629, 1694, 1704 and 1642 cm^{-1}, and 1344, 1330, 1332 and 1301 cm^{-1}, respectively. The aromatic C-H bonds displayed the weak bands at 3020, 3068, 3066, 3062, 3100 and 3112 cm^{-1} beside the in-plane bending deformation mode of vibration at 1480, 1442, 1442, 1398 and 1442 cm^{-1} for Fe, Co, Ni, Zn and La metal-complexes, respectively. The νC-S-C band appeared the bands at 688, 678, 696, 698, 688 and 704 cm^{-1}. The coordination bond M$\leftarrow$ N was noticed by the bands at 614, 616, 542, 490, 470 and 552 cm^{-1}.

For III_{a-f}, the coordinated water molecules associated with the complex exhibited the weak broad bands at 3346, 3456, 3354, 3370, 3368 and 3428 cm^{-1}. The aliphatic C-H bond in the azomethine group, and the acetate groups in Fe, Co, Ni, Cu, Zn and La metal-complexes was assigned to the weak broad bands observed at 2975, 2940, 2936, 2926, 2932 and 2952 cm^{-1}. Similar to the aforementioned, the νC=N bond in the azomethine group demonstrated the bands at 1518, 1532, 1528, 1518, 1522 and 1570 cm^{-1}. The ν_{as} COO^- and ν_{sym} COO^- of Ni, Cu and Zn metal-complexes located at 1694, 1600 and 1602 cm^{-1}, and 1336, 1338 and 1338 cm^{-1}, respectively. The aromatic C-H bond exhibited the weak bands at 3034, 3065, 3044, 3064, 3058 ,1448 and 3180 cm^{-1}, and the in-plane bending deformation mode of vibration at 1398, 1440 and 1468 cm^{-1} in the spectra of Fe, Co, Ni and La, respectively. The appearance of the bands located at 694, 682, 692, 698, 698 and 688 cm^{-1} was attributed to the νC-S-C. Finally, the bands at 594, 614, 543, 538, 538 and 618 cm^{-1} were accounted for the coordination bond M$\leftarrow$ N.

Molar conductance

The molar conductance of the complexes was measured in DMF solution of 10^{-3}M at room temperature. The metal-complexes of Fe, Co, Ni, Cu, Zn and La, I_{a-f}, respectively revealed 44.1, 8.5, 38.6, 14.7, 1.8 and 90.6 Ω^{-1} cm^2 mol^{-1}. Meanwhile, II_{a-f} showed the molar conductance yields of 52.7, 12.6, 10.3, 38.6, 8.0 and 43.2 Ω^{-1} cm^2 mol^{-1} and the obtained results for III_{a-f} in similar order were 78.5, 18.6, 16.7, 25.2, 10.2 and 396 Ω^{-1} cm^2 mol^{-1}. The shown remarkable low values of I_{a-e}, II_{b-f} and III_{b-e} suggest the including of the associated anions in the coordination sphere of the metal-complex, indicating the non-electrolyte behavior. Further, the results of I_f, II_a and III_a showed 1:2 electrolyte behavior, suggesting the ionic nature.

UV-Visible and magnetic behavior: coordination geometry

The magnetic properties of the metal-complexes, as a result of the isolating effect of the ligand yield direct information on the electronic configuration of the central ions, oxidation state of metal ion and the number of the unpaired electrons of the d-shell.

The UV spectra of the metal-complexes exhibited absorption bands within λ_{max} = 202-247 nm and λ_{max} = 250-259 nm that correspond to ($^1L_a \leftarrow {}^1A$) and ($^1L_b \leftarrow {}^1A$) transitions of the ligand phenyl ring. Meanwhile, the bands at λ_{max} = 268-286 nm correspond to the π-π* transition while the bands at λ_{max} = 302-332 nm represent the n-π* transition of the C=N in the azomethine group. The d-d transitions appeared within λ_{max} = 367-797 nm.

The measured magnetic moment of Fe (III)-complexes I_a, II_a and III_a, μ_{eff} = 5.03-6.02 B.M., suggested the octahedral, high-spin, geometry. The coordination geometry was supported by three bands within λ_{max} =367-606 nm that are assignable for $^6A_1 \rightarrow {}^4T_1$ (G), $^6A_{1g} \rightarrow {}^4E_g$, $^4A_{1g}$ (G) and $^6A_{1g} \rightarrow {}^4E_g$ (D) transitions.

Both tetrahedral and high-spin octahedral Co (II)-complexes I_b, II_b and III_b possess three unpaired electrons, however, they may be distinguished by the magnitude of deviation of μ_{eff} from the spin-only value [25]. The measured magnetic moment, μ_{eff} = 4.0-4.41 B. M., shades light on the presence of three unpaired electrons indicating a high-spin octahedral configuration. This is supported by the band within the region λ_{max} =356-441 nm representing the $^4T_1g \rightarrow {}^4T_1g$ (P) transitions in I_b and II_b complexes. Meanwhile, III_b exhibited a band within the region λ_{max} =375-427 nm interpreted for $^4A_2$ (F) $\rightarrow {}^4T_1$ (P) transition confirming a tetrahedral configuration.

The measured magnetic moment for Ni (II)-complexes I_c, II_c and III_c, μ_{eff} = 2.84-3.18 B.M., is of high-spin at room temperature and consistent within the observed normal range for octahedral Ni (II)-complexes.[26] The suggested configuration is supported by the appearance of three bands within the region λ_{max} =375-498 nm in II_c and III_c As the ground state of Ni (II) in an octahedral coordination is $^3A_{2g}$, the exhibited bands may be assigned to the $^3A_{2g}(F) \rightarrow {}^3A_{2g}$ (P) transition.

The measured magnetic moment for Cu (II)-complexes I_d, II_d and III_d, μ_{eff}= 1.7-1.85 B. M., at room temperature is consistent within the range normally observed for distorted octahedral [27]. The ^2E_g and $^2T_{2g}$ states of the octahedral Cu^{+2} ion (d^9, ^2D term) split under the influence of the tetragonal distortion due to ligand field and Jan-teller distortion effect.[28] By distortion three spin allowed transitions are expected: $^2B_{1g} \rightarrow {}^2A_{1g}$, $^2B_{1g} \rightarrow {}^2B_{2g}$ and $^2B_{1g} \rightarrow {}^2E_g$. The Cu-complexes I_d, II_d and III_d displayed bands in the region λ_{max} =375-500 nm referred to $^2B_{1g} \rightarrow {}^2B_{2g}$ and $^2B_{1g} \rightarrow {}^2E_g$ transitions. The Zn- and La-complexes are diamagnetic possessing the octahedral coordination. Measured magnetic moments are tabulated in Table (5)

Table 5: The magnetic properties of the metal Schiff-base complexes

Complex		μ_{eff} (B. M.)
.No	Metal	
I_a	Fe	5.4
I_b	Co	4.41
I_c	Ni	2.84
I_d	Cu	1.78
I_e	Zn	Diamagnetic
I_f	La	Diamagnetic
II_a	Fe	5.67
II_b	Co	4.00
II_c	Ni	3.18
II_d	Cu	1.82
II_e	Zn	Diamagnetic
II_f	La	Diamagnetic
III_a	Fe	5.03
III_b	Co	4.31
III_c	Ni	2.93
III_d	Cu	1.83
III_e	Zn	Diamagnetic
III_f	La	Diamagnetic

^{1}H NMR spectra

^{1}H NMR spectra of Zn-complexes, I_e, II_e and III_e, were recorded in DMSO-d_6. The signal appeared at δ 9, 8.8 and 8.4, respectively, was of lesser intensity than seen for the azomethine proton in the ligands. The multiplet signals at δ 7-7.6 in I_e and II_e spectra and at δ 7.1-7.9 in III_e spectrum are attributed to the aromatic protons in the two different phenyl rings. The acetate methyl proton displayed a signal at δ 1.83, 1.86 and 1.85, respectively.

In view of the spectral arguments the following conformations may be allowable for the metal-complexes I_{a-f}, II_{a-f} and III_{a-f} .

where,

I_a; M= Fe^{3+}, X=NO_3
I_f; M= La^{3+}, X=Cl

I_b; M= Co^{2+}, X=Aco
I_c; M= Ni^{2+}, X=Aco
I_d; M= Cu^{2+}, X=Aco
I_e; M= Zn^{2+}, X=Aco

where,

II_a; M= Fe^{3+}, X=NO_3
II_f; M= La^{3+}, X=Cl

II_b; M= Co^{2+}, X=Aco
II_c; M= Ni^{2+}, X= Aco
II_d; M= Cu^{2+}, X=Aco
II_e; M= Zn^{2+}, X=Aco

where, II_b

II_a; M= Fe^{3+}, X=NO_3
II_f; M= La^{3+}, X=Cl

where,

II_c; M= Ni^{2+}, X=Aco
II_c; M= Co^{2+}, X= Aco
II_d; M= Cu^{2+}, X=Aco
II_e; M= Zn^{2+}, X=Aco

Miscellaneous behaviors

γ- Irradiation stability

γ- irradiated of ligand10^{-5}M in DMF solutions was conducted at conditions of: =30kGy total integratal dose ,1.2 Gy s^{-1} dose rate, neutral medium, and ambient air and room temperature. The applied dose rate of relatively low linear energy transfer favors the non-interradical reactions (29). Further, the excitation energy received by the aromatic systems is channeled to relatively low-energy triplet excited states which have a low probability of dissociation (30). This is also confirmed for nitrobenzene as radiolysis yields which are low compared with nitromethane(31). Nevertheless, the presence of the aromatic ring does not stabilize the aromatic halide. This is mainly due to electron scavenging with formation of an aromatic radical and a stable halide ion that may be later converted to a halogen atom during ion neutralization [32]. Analogues to the γ- radiolysis of acetone at a relatively low dose rate, 0.81 Gy s^{-1}, DMF methyl radicals may produce similar products, e.g. H_2, H_4 and CO, and also attack the substrate giving various yields [33].

Generally, the impact of irradiation was explicitly noticed in the resolution of the fingerpoint of the ligands I, II, III. Contrarily, the phenylic transition region within λ_{max} =200-260 nm, revealed better and numerous resolved species, whereas, within λ_{max} =260-320 nm, less resolved and larger absorbance features were detected in association with the disappearance of the C=N n-π^* transition at 330 nm. This may shade light on the generation of various aromatic structures in addition to the formation of longer and diverse conjugated systems as a result of change in the azomethine bond and the likelihood of aromatic radical- radical recombinations. Simulating the MS yields, as a first approach, three potential radiolysis products may be suggested [34]:

Postulated radiation- induced species

The metal-complexes $I_{a\text{-}d}$ and $II_{a\text{-}d}$ displayed rather similar behaviors within the region λ_{max} = 200- 340 nm where the phenylic transitions exhibited much lesser absorbance with better resolution, whereas the π-π^* transition sector showed better resolution, whereas the π-π^* transition sector showed distortion in the structure with slight decrease in the general absorbance. On the other hand in the case of the metal-complexes $III_{a\text{-}d}$, the region of the phenylic transitions demonstrated steadiness in absorbance with obvious decrease and distortion in the π-π^* transition sector. This may suggest that a fragmentation in the conjugated systems took place as a result of methyl radical attack aided by the withdrawing group NO_2.

In the visible region at a concentration of 10^{-3} M, I_a gave two strong bands at λ_{max} = 367 and 581 nm characterizing the presence of Fe (III) ion. By γ-irradiation the two bands completely disappeared suggesting the decomposition of the coordination structure. Similar observation was reported for I_b and I_c within the region λ_{max} = 350-450 nm. Meanwhile, I_d showed some bands in the region λ_{max} = 350-500 nm that turned out much less resolved by irradiation, probably by the generation of various species. Less resolved but persistent shapes were also noticed in the region λ_{max} = 350-500 nm by irradiating II-and III-complexes.

It is evident that, distortion of the complex structure by irradiation definite at the applied conditions resulting in the formation of several structures [35].

Thermal stability

The Fe-complex I_a exhibited a four-staged thermogram. A weight loss of 3.74% at 130 ºC was accounted for one molecule of the coordination water. Two next steps showed weight loss of 11.41 and 11.8%, respectively, within the ranges 130-220 ºC and 220-350 ºC, referred to two NO_3 groups. A last weight of 30.08% within the region 350-620 ºC was assigned for $[C_7H_6NO_3]$ adducts. The residue of 41.8% could withstand to 1000 ºC.

Three decomposition stages were observed for II_d started by 6.01% weight loss within the range 100-160 ºC ascribed to ≈ two molecule of the coordination water. The second weight loss was 20.67 % within the range 160-390 ºC attributed to two acetate groups. The last stage within the region 390-870 ºC was of 56.63% accounted for $[C_{16}H_{11}Cl\ NS]$ adduct. The residue of 15.5 % corresponds to the molecular weight 79.8 may be determined for a CuO molecule.

The metal-complex III_c demonstrated a four-staged thermal decomposition. A weight loss of 2.83% at 150 ºC was attributed to one molecule of the coordination water. Within the range 170-320 ºC a weight loss of 13.8% was referred to one acetate group and a nitrogen half-molecule. A weight loss of 15.32% followed within the region 320-420 ºC ascribed to a separation of one benzene molecule. The last loss was 61.4% within the range 420-870 ºC determined for $[C_{16}H_{11}N_3O_2S]$ adduct. A residue of 6.23% proved thermal stability up to 1000 ºC.

Antimicrobial activity

The synthesized metal-complexes were tested, using ampicillin as a reference, while dissolved by 1g/ml DMSO. Against the Gram-positive Bacillus *subtilis* (NCTC-1040), III_d showed very high activity, whereas II_b showed significant inhibition; II_d revealed moderate inhibition, and I_{a-c} and $III_{b,e}$ exhibited weak inhibition. Further, against Streptococcus *pyogenes* (ATCC-19615), II_b showed significant inhibition, whereas II_d and III_{b-d} revealed weak inhibition.

The Gram-negative bacteria displayed the following: for E. *coli*, I_c showed significant inhibition, whereas II_b revealed moderate inhibition and $III_{b,c}$ gave weak results. For Clostridium, I_c and III_d showed only weak inhibition.

The metal-complexes were also tested for the antifungal activity using Clofran as a reference. For Aspergillus *fungatus*, II_b showed significant inhibition whereas III_d revealed moderate activity.

Conclusions

The elemental and spectral analyses confirmed the proposed chemical structures of the synthesized Schiff-bases I, II and III and metal-complex derivatives I_{a-f}, II_{a-f} and III_{a-f}. The broadness and shift to lower IR frequencies of the azomethine group evidenced the role of the group in the coordination process. The involvement of coordination water in the coordination sphere was also asserted by the TGA results. The UV-Visible spectra reported data in association with the magnetic behavior of metal-complexes suggested the dominance of the octahedral arrangement except Cu-complexes which displayed distorted octahedral geometry.

The γ-irradiation process revealed rather stronger influence on the metal-complexes than the parent ligands indicating lesser radiation stability behavior of the coordination arrangement. The radiolysis of the ligand and metal chelates substrates as well as the employed solvent was discussed and some presumably formed species were postulated.

The molar conductance values of the metal-complexes suggest the non-electrolytic behavior and the involvement of the acetate group, in the acetato complexes, in the coordination sphere. The molar conductance results indicated also the 1:1 electrolyte behavior in the case of I_f, II_a and III_a and the 1:2 electrolytes to III_f suggesting the ionic nature. On the other hand, some metal-complexes demonstrated substantial antibacterial and antifungal activities. The Cu-complex III_d has been proved to be very highly active against Bacillus *subtilis* in reference with ampicillin.

References

1. P. Vicini, F. Zani, P. Cozzini, I. Doytchinova, Eur. J. Med. Chem. 37, 553. (2002).
2. A. Geronikaki, A. Lagunin, V. Poroikov, D. Filimonov, D. J. Hadjipavlou-Litina, P. Vicini, SAR QSAR. Environ. Res. 13, 457 (2002).
3. P. Vicini, L. Amoretti, V. Ballabeni, M. Tognolini, E. Barocelli, Bioorg. Med. Chem. 8, 2355 (2000).
4. P. Vicini, C. Manotti, A. Caretta, L. Amoretti, Arzneim.- Forsch./Drug Res. 49, 896 (1999).
5. D. J. Hadjipavlou-Litina, A. Geronikaki, Drug Des. Discov. 15, 199 (1998).

6. P. Vicini, C. Manotti, A. Caretta, L. Amoretti, Arzneim.- Forsch./Drug Res. 47, 1218 (1997)
7. A. Combes, Compt. Rend., 168, 1252 (1889).
8. N. F. Curtis, J. Chem. Soc., 4409 (1960).
9. N. F. Curtis and D.A. House, Chem. Ind. (London) 1708 (1961).
10. M. M. Blight and N. F. Curtis, J. Chem. Soc. 12904 (1962).
11. M. M. Blight and N. F. Curtis, J. Chem. Soc. 2016 (1962).
12. C. Bi. Y. Fan, G. Sun, G. Zheng and G. Zhang, Synth. React. Inorg. Met.-Org., Chem., 31, (2), 219 (2001).
13. P. Vicini, A. Geronikaki, M. Incerti, B. Busonera, G. Poni, C. A. Cabrasc and P. L. Colla, J. Bioorg. Med. Chem. 11, 4785–4789 (2003)
14. Sakyan, E. Logoglu, S. Arslan, N. Sari, N. Sakiyan, Bio Metals 17, 115 (2004).
15. R. C. Sharma, V. K. Varshney, J. Inorg. Biochem. 41, 299 (1999).
16. P. Vicini, A. Geronikaki, M. Incerti, B. Busonera, G. Poni, C. A. Cabrasc, P. L. Collac, Bioorg. Med. Chem. 11, 4785 (2003).
17. W. T. Gao and Z. Zheng, Molecules 7, 511 (2002).
18. M. L. Colon, S. Y. Qian, D. Vanderveer and X. R. Bu, Inorg. Chim. Acta 357, 83 (2004).
19. A. Ciobanu, F. Zalaru, C. Zalaru, F. Dumitrascu and C. Draghici, Acta Chim Slov. 50, 441 (2003).
20. X. Tai, X. Yin, Q. Chen and M. Tan, Molecules 8, 439 (2003).
21. Chalt and H. R. Waston, J. Chem. Soc. 2, 545 (1962).
22. F. Bates, "Modern Magnetism" 2nd edit. Cambridge at the university press (1948).
23. W. Hewitt, S. Vincent, “theory and application of microbiological array” publishes Academic press, INC. New York (1989).
24. S. A. El-Enein, F. A. El-Ssaied, S. M. Ell-Salamony, J. Spectrochimica Acta Part A, 71,421-429 (2008).
25. R. Schlapp, W. G. Penney, Phys. Rev. 42 (1932)286
26. F. A. Cotton, G. Wilkinson, in: Advanced Inorganic Chemistry (Wiley Interscience), New York, 5th ed., (1988) 725.
27. R. S. Kumar, M. Nethiji, K. C. Patil, polyhedron 10 (1991) 365
28. G. L. Miessler, D. A. Tarr, in: Inorganic Chemistry (3rd d), Pearson Prentice Hall (2004).
29. J.H.Baxendale and P.Wardman, u.s. Dept. Commerce- National Bureauf Standards, Washington, DC. (1975)

30. W.G. Burns and R. Barker in Aspects of Hydrocarbon Radiolysis (eds.T. Gaumann and J.Hoigne), Academic,NY, ch.2.(1968)

31. J. A. Knight, Radiat.Res, 52, 17 (1972)

32. J. W. Buchanan and R. J. Hanrahan, Radiat.Res. , 44,305(1970)

33. E. P. Grimsrud and P. Kebarle, J. Am.Chem. Soc, 95, 7939(1973)

34. A. M. Dessouki, N. B. El-Assy, R. O. Aly, E.H. M. Ibrahim and M. M. El- Dossouky, J. Rad. Nucl. Chem., 100(1), 49 (1986)

35. R. O. Aly, I. M. Abd-Ellah, R. S. Farag, and M. M. Hassan, Al-Azhar Bull. Sci. (AISC ′08), 61-70 (March 2008).